A&A 405, L19–L22 (2003)
DOI: 10.1051/0004-6361:20030760

Astronomy & Astrophysics

Discovery of a $z = 6.17$ galaxy from CFHT and VLT observations⋆

J.-G. Cuby[1], O. Le Fèvre[2], H. McCracken[3], J.-C. Cuillandre[4], E. Magnier[4], and B. Meneux[2]

[1] European Southern Observatory, Paranal, Casilla 19001, Santiago 19, Chile
[2] Laboratoire d'Astrophysique de Marseille, France
[3] Osservatorio Astronomico di Bologna, Italy
[4] Canada-France-Hawaii Telescope Corporation, Hawaii, USA

Received 1 April 2003 / Accepted 19 May 2003

Abstract. We report the discovery of a galaxy at a redshift $z = 6.17$ identified from deep narrow band imaging and spectroscopic follow-up in one of the CFHT-VIRMOS deep survey fields at 0226-04. In addition to the existing deep *BVRI* images of this field, we obtained a very deep narrow band image at 920 nm with the aim of detecting Lyα emission at redshift ~6.5. Spectroscopic follow-up of some of the candidates selected on the basis of their excess flux in the NB920 filter was performed at the VLT-UT4 with the FORS2 instrument. For one object a strong and asymmetric emission line associated with a strong break in continuum emission is identified as Lyα at $z = 6.17$. This galaxy was selected from its continuum emission in the 920 nm filter and not from its Lyα emission, in effect performing a Lyman Break detection at $z = 6.17$. We estimate a star formation rate of several tens of $M_\odot\,\mathrm{yr}^{-1}$ for this object, with a velocity dispersion ~400 km s^{-1}. The spectroscopic follow-up of other high z galaxy candidates is on-going.

Key words. galaxies: high-redshift – early Universe – techniques: spectroscopic

1. Introduction

Recent observations of galaxies at redshifts >5, and more recently >6 have been reported. These observations follow a well defined observing strategy based on Lyα searches at increasing wavelengths in low OH emission sky windows (see e.g. Hu et al. 2002; Cuby et al. 2002; Rhoads et al. 2003; Kodaira et al. 2003; Lilly et al. 2003) and/or on Lyman Break detection in the RIz bands (e.g. Lehnert & Bremer 2003). The Sloan Digital Sky Survey has in the meantime unveiled a large number of $z > 5$ QSO's (Fan et al. 1999; Anderson et al. 2001) from Lyman break detection.

These recent observations have generated extensive debates in the literature regarding a possible redshift of the reionization of the Universe at $z \approx 6$ (see e.g. Becker et al. 2001; Hu et al. 2002; Lehnert & Bremer 2003 and references therein). In February 2003 the publication of the WMAP results (Bennett et al. 2003) has shed new light on the early epochs of the Universe, in particular in dating the epoch of the reionization at $11 < z < 30$. This suggests that the current observational limit at $z \approx 6.5$ corresponds to an epoch significantly beyond the re-ionization period and that previous failures and recent success in detecting $z > 6$ objects are due to the evolution of the search techniques more than to the ionization state of the IGM at this redshift. However various models of the reionization phases of the Universe by massive stars, miniquasars or neutrinos allow to reconcile the $z \sim 6$ Gunn-Peterson trough observations with the WMAP data (Haiman & Holder 2003; Hansen & Haiman 2003; Cen 2003). The detectability of the Lyα emission line for a galaxy embedded in a neutral IGM is discussed in Haiman (2002).

We report in this letter the discovery of a $z = 6.17$ galaxy discovered from Narrow Band imaging performed at CFHT and follow-up spectroscopy at the VLT. In Sect. 2 we present the observations and in Sect. 3 the results which are briefly discussed in Sect. 4.

We assume in the following a cosmology based on the most recent values derived from WMAP data, i.e. $H_0 = 71$ km s^{-1} Mpc^{-1}, $\Omega_{\mathrm{matter}} = 0.27$ and a flat Universe.

2. Observations

2.1. Imaging and object selection

We have obtained deep Narrow Band imaging at 920 nm with the CFH12K CCD mosaic (Cuillandre et al. 2000) during 4 nights in November 2001. The selected field at 0226-04 is one of the VIRMOS-VLT Deep Survey (VVDS) fields (Le Fèvre et al. 2001) for which deep photometric catalogs from broad

Send offprint requests to: J.-G. Cuby, e-mail: jcuby@eso.org

⋆ Based on observations collected at the Canada-France-Hawaii Telescope operated by the National Research Council of Canada, the Centre National de la Recherche Scientifique de France and the University of Hawaii (Programme 01BF1) and on observations collected at the European Southern Observatory, Paranal, Chile (ESO Programme 70.A-0513).

band *BVRI* data obtained with the same instrument were already available. The existing *BVRI* data reach limiting magnitudes of $I_{AB} = 25.3$ for a 3σ detection in a 3 arcsec circular aperture (McCracken et al. 2003). The field of view is $28' \times 42'$ with $0.2''$ sampling. Conditions were photometric. In total 20 hrs of integration were accumulated at a median airmass of 1.22 with individual exposure times of 900 s.

The NB920 filter was designed with a central wavelength 920 nm and a 10 nm bandwidth to match a region of low sky emission between OH lines. The measured background level was ~ 1 e$^-$ s^{-1} pixel^{-1} providing background limited observations. The resulting image quality on the combined image is $\sim 0.8''$ with some slight image elongation ($\sim$10%) due to oscillations of the declination axis of the telescope.

The 80 dithered images were centered and stacked after standard pre-processing: bad pixel masking, dark correction and (twilight) flat-fielding and fringe subtraction. The stacked image was then distortion corrected, astrometrically calibrated and matched to the *BRVI* images of the field. Some residual fringing persisted, which was further removed chip by chip by a 50 order spline 3 fitting.

Object detection on the NB920 image was then performed chip by chip with SExtractor (Bertin & Arnouts 1996). Careful visual inspection allowed to further remove false detections, in particular in the regions of poor cosmetic quality and/or of overlap between the chips of the mosaic. For all remaining objects the photometry of the χ^2 *BVRI* VIRMOS detection image (McCracken et al. 2003) was measured using DAOPHOT under IRAF. The final selection was performed by keeping all objects for which the *BVRI* flux was below an arbitrary low level. Thumbnails of the fields around each candidate were extracted and visual inspection further allowed to remove remaining false and/or ambiguous detections.

2.2. Spectroscopy

Spectra of some candidates were obtained at the VLT with FORS2 using the 19 movable slitlet capability of the instrument, with slit widths of $2''$ and a pixel scale of $0.25''$. The seeing conditions were in average of the order of 0.8–$1.0''$. In total, 3 fields and approximately 30 candidates were observed in a combination of service and visitor mode observations from November 2002 to January 2003. The combination of a MIT/LL CCD mosaic with a holographic grism provides extremely good performance up to 1 μm with little fringing. The setup used provides a reciprocal dispersion of 1.6 Å pixel^{-1} giving a spectral resolution in the range 700–1400 depending on the size of the objects through the $2''$ slits.

Observations on each field consisted of 1.9 hr of integration time split in 6 exposures with dithering along the slits. After flat fielding, running skies were generated for each frame from the 5 other frames. The sky subtracted frames were then distortion corrected, registered and stacked, and sky line residuals were removed by column fitting.

One target was clearly identified on the resultant 2D combined images as a high redshift galaxy by the presence of a strong, asymmetric emission line and a strong continuum break

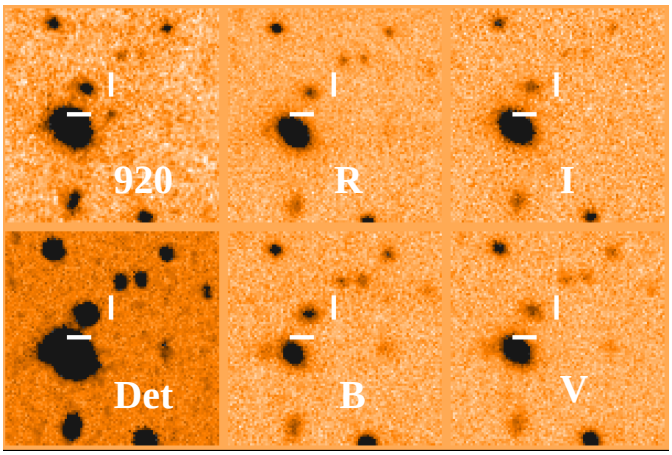

Fig. 1. Thumbnail images of the field of view in *BVRI*, 920 nm images around the target. "Det" indicates the detection image computed from the χ^2 sum of the individual *BVRI* stacks (McCracken et al. 2003). The thumbnails are $20''$ on a side. East is right, North is up.

across the line. The total spectral coverage for this object is 762–1091 nm. The emission line lies at shorter wavelength than in the expected 920 nm window: the relatively strong continuum caused instead this object to be detected in the NB920 image and be selected for its continuum Lyman break.

Results for this particular object are presented in this letter, while the analysis of the imaging and spectroscopic data for the full sample will be presented in a subsequent paper.

3. Results

3.1. Imaging

Figure 1 shows *BVRI* and NB920 thumbnail images around the object. The object is unresolved at the spatial resolution of the image ($\sim 0.8''$).

Flux calibration was performed on a number of standard fields, SA111, SA113 and MarkA. In total 9 stars were used in the 3 fields to derive the photometric zero point at 920 nm. Furthermore, 2 of these 3 fields were dithered across the mosaic, allowing to characterize the sky concentration and scattered light patterns and to construct a photometric superflat correction map. The 920 nm magnitudes were derived by an ad hoc extrapolation of the *BVRI* magnitudes of the 9 standard stars leading to *I* band magnitude corrections of ± 0.1 to 0.5. In spite of the uncertainties associated to this process, the resulting statistical errors turned out to be <0.1 mag peak to peak. The measured magnitude for the object is NB920 = 23.77, corresponding to a flux density of $\sim 2.6 \times 10^{-19}$ ergs s^{-1} cm^{-2} Å^{-1}.

3.2. Spectroscopy

Figure 2 shows the 2D spectrum of the galaxy as observed with FORS2. The total absence of continuum detection blueward of the line is consistent with the non detection of the object in the *R* image. The non detection in the *I* band image is further discussed below.

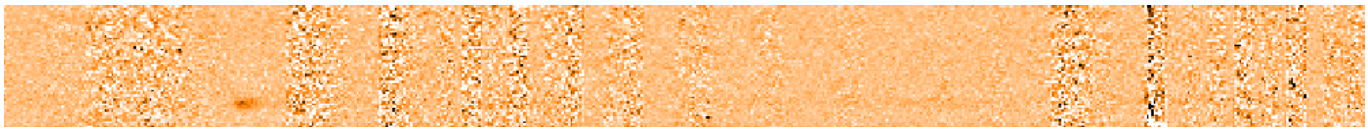

Fig. 2. 2D spectrum. The emission line is clearly visible, with its asymmetric profile, and the continuum is visible throughout the 920 nm OH free window. Wavelength increases linearly to the right from 857 to 955 nm.

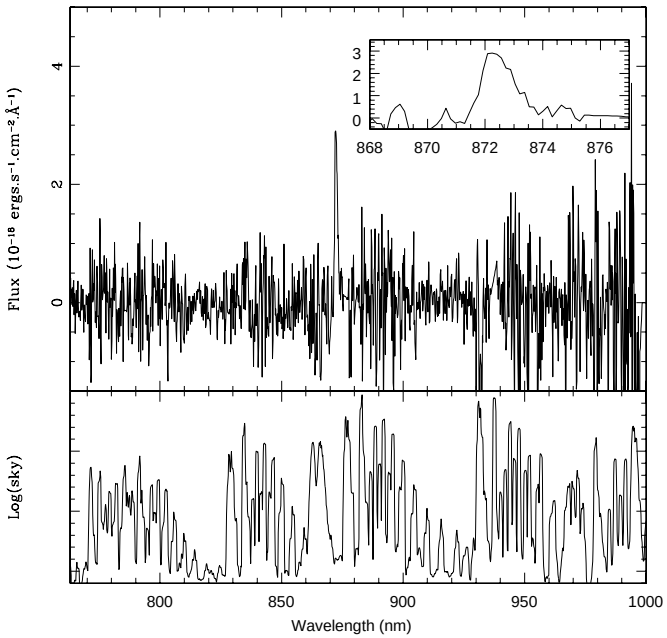

Fig. 3. Extracted spectrum in the range [760–1000] nm, with a close-up view of the emission line in the range [868–877] nm. The sky spectrum is shown in arbitrary logarithmic units.

Flux calibration was done from observation of a standard star (LTT3218) observed through a 5″ aperture located at the center of the field of view of the instrument and covering the spectral range 731–1059 nm. The spectral range common to the object and the standard star is therefore [762–1059] nm. The resulting flux calibrated spectrum is shown in Fig. 3.

The line peaks at 872.3 nm. We measure a line intensity of 3.9×10^{-17} ergs s^{-1} cm^{-2} with a cumulated error (slit losses, spectrophotometric calibration, measurement errors and signal to noise) estimated to be less than 20% (3σ).

The continuum, although at a $S/N \sim 1$ per pixel could be estimated with good accuracy by fitting the spectroscopic 2D frame (Fig. 2) along the dispersion direction in selected low noise windows (before and after the line).

We measure a mean flux density of $0. \pm 3 \times 10^{-20}$ ergs s^{-1} cm^{-2} Å^{-1} ($3\ \sigma$) in the range 809–828 nm and $\sim 2.4 \pm 0.6 \times 10^{-19}$ in the range 914–928 nm (corresponding to the NB filter), in excellent agreement with the CFH12k NB920 photometry. The amplitude of the continuum break across the emission line is therefore >8 or >2.3 mag.

We have examined several possibilities for the emission line: Hα at $z = 0.329$, [OII] at $z = 1.340$ or $z = 6.17$ for Lyα. The identification with Lyα is the most likely on the basis of the following arguments.

First, the strong continuum break across the line is only compatible with Lyα. We have examined a complete set of simulated spectra produced with GISSEL (Bruzual & Charlot 1993), spanning a range of burst age from 0.01 to 12 Gyr, and metallicities from 0.004 to solar. The amplitude of the continuum break never exceeds 1.8 mag for [OII] and only for models with old stellar populations unlikely to exhibit [OII] in emission, it is 0.2–0.3 mag around Hα while it can easily exceed 2−3 mag around Lyα.

Second, the equivalent width at rest also favors identification with Lyα. From the averaged continuum under the line we derive rest frame equivalent widths of ∼50 Å for Lyα, 150 Å for [OII] and 270 Å for Hα. A value of 150 Å is at the extreme end of the distribution for [OII] at redshifts ∼1 (Hammer et al. 1997), a value of 270 Å has never been observed for Hα at low redshifts (Tresse et al. 1996), while the value for Lyα is quite common at high redshifts (Steidel et al. 1999; Hu et al. 2002; Rhoads et al. 2003).

Finally, the line is clearly asymmetric (see Fig. 3), as typical of Lyα at high redshifts with a sharp fall-off in the blue due to interstellar and/or IGM absorption.

We conclude that the most likely identification of the observed emission line is Lyα at $z \sim 6.17$, by slightly underestimating the redshift derived from the line peak to account for a likely typical distortion of the Lyα line on its blue side.

The observed line width is 13 Å. Since the object is not resolved in imaging (in the UV continuum above Lyα), we assume that the instrumental profile is given by the seeing disk, i.e. ∼0.8″ as measured across the trace of bright objects in the same frame. This leads to a velocity dispersion ∼400 km s^{-1}.

From the flux measurements above, we can verify a posteriori the integrated I band magnitude for this object. Assuming that the continuum level is constant above the Lyα line and nil below and taking into account the decrease in CCD quantum efficiency across the I band we derive for our object $I_{\rm AB} \sim 25.9$. At this magnitude the completeness limit of our I band image is ∼50% (McCracken et al. 2003), confirming a posteriori that this object may not be visible in the I band image (see Fig. 1).

The measured properties of our object are summarized in Table 1.

4. Discussion

Observation of objects at the highest redshifts is critical for our understanding of the formation and evolution of the galaxies and of the early phases of the Universe. Although we examine only one such object, it is of interest to assess its properties.

Table 1. Properties of our 6.17 galaxy. [1]: rest frame, [2]: observed frame.

Alpha (2000)	Delta (2000)	NB920 mag	Lyα[2] nm	*FWHM* nm[2]	*FWHM* km s^{-1}	*EW*[1] Å	F(Lyα)[2] 10^{-17} ergs s^{-1} cm^{-2}	F(127.5.–129.4 nm)[2] 10^{-19} ergs s^{-1} cm^{-2} Å^{-1}
02:28:02.97	−04:16:18.3	23.77	872.3	1.3	400	50	3.9	2.5

Classical estimators of the star formation rates (Kennicutt 1998) from the Lyα luminosity (assuming case B recombination) and UV continuum flux (although used here at shorter wavelengths than the recommended 1500–2800 Å range) give for our object and for our assumed cosmology SFR(Lyα) = 15 $M_\odot\,\mathrm{yr}^{-1}$ and SFR(UV) = 60 $M_\odot\,\mathrm{yr}^{-1}$. The higher rate SFR(UV), albeit similar to SFR(Lyα) within the uncertainties of the estimators, is not unusual and could reflect the effects of dust absorption on the Lyα photons in the interstellar and intergalactic medium. This SFR is similar to the values derived from other high-z galaxy observations Kodaira et al. (2003); Hu et al. (2002); Rhoads et al. (2003).

Our measurements indicate a strong velocity field of several hundreds of km s^{-1}, which might be related to the inflow of gas onto a recently formed, or being assembled, galaxy. As for the brightness of the line, it is however important to note that this value is a lower limit of the actual line width.

All existing observations of high redshift galaxies indicate moderate to vigorous star formation rates. The WMAP dating of the re-ionization of the Universe (Kogut et al. 2003) indicates that the first stars were born very early in the Universe, before the first 400 Myr. Objects ∼0.9 Gyr old ($z \sim 6.5$) may therefore have already experienced several cycles of star formation and metal enrichment, as observed in $z > 6$ SDSS quasars (Pentericci et al. 2002) and 1.5 Gyr later at redshift 2.7 in a Lyman break galaxy (Pettini et al. 2002). Conversely, the high *EW* of Lyα in the high-z galaxies observed so far rather point to low metallicity objects. The strong Lyα luminosity of $\sim 1.7 \times 10^{43}$ ergs s^{-1} determined for our object may imply a young object (Lehnert & Bremer 2003).

Short of higher *S/N* spectroscopy at higher wavelengths, it is difficult to infer the metallicity of the few high z galaxies known. Clearly more $zJHK$ observations are required to better determine the nature and chemical composition of these distant galaxies, and to compare them with quasars at the same redshifts or LBG's at lower redshifts.

We defer to a later paper the analysis of the space density of high redshift galaxies based on the CFHT and VLT-FORS2 observations of our complete sample of NB920 candidates.

5. Conclusion

We report in this letter the discovery of a field galaxy at redshift 6.17 as part of a dedicated narrow band imaging search for $z \sim 6.5$ galaxies. We note that our object was discovered through its UV continuum emission and not through its Lyα emission, indicating that deep imaging on 4 m class telescopes can indeed turn out $z \sim 6$ objects from continuum detection.

Similar dedicated high-z galaxy searches are now consistently reporting discoveries of $z > 6$ objects, i.e. less 1 Gyr old objects, undergoing moderate to high star formation.

Larger samples are required to understand how galaxies evolve through this important epoch in the life of the Universe.

Acknowledgements. We thank S. Arnouts for providing the GISSEL simulations mentioned in text, the anonymous referee for useful comments, the CFHT and ESO staff at Paranal and Garching for their always efficient and dedicated support and the time allocating committees for granting us observing time.

References

Anderson, S., Fan, X., Richards, G., et al. 2001, AJ, 122, 503
Becker, R., Fan, X., White, R., et al. 2001, AJ, 122(6), 2850
Bennett, C., Halpern, M., Hinshaw, G., et al. 2003, ApJ, submitted [astro-ph/0302207]
Bertin, E., & Arnouts, S. 1996, A&AS, 117, 393
Bruzual, A., & Charlot, S. 1993, ApJ, 405, 538
Cen, R. 2003, ApJ, submitted [astro-ph/0210473]
Cuby, J.-G., Le Fèvre, O., McCracken, H., et al. 2002, in Proc. SPIE, 4834
Cuillandre, J.-C., Luppino, G., Starr, B., & Isani, S. 2000, in Proc. SPIE, 4008, 1010
Fan, X., Strauss, M., Schneider, D., et al. 1999, AJ, 118, 1
Haiman, Z. 2002, ApJ, 576, L1
Haiman, Z., & Holder, G. 2003, ApJ, submitted [astro-ph/0302403]
Hammer, F., Flores, H., Lilly, S., et al. 1997, ApJ, 481, 49
Hansen, S., & Haiman, Z. 2003, ApJ, submitted [astro-ph/0305126]
Hu, E., Cowie, L., McMahon, R., et al. 2002, ApJ, 568(2), L75
Kennicutt, R. 1998, ARA&A, 36, 189
Kodaira, K., Taniguchi, Y., Kashikawa, N., et al. 2003, PASJ, 55
Kogut, A., Spergel, D., Barnes, C., et al. 2003, ApJ, submitted [astro-ph/0302213]
Lehnert, M., & Bremer, M. 2003, ApJ, accepted [astro-ph/0212431]
Lilly, S., Tran, K.-V., Brodwin, M., et al. 2003, ApJ, submitted [astro-ph/0304376]
Le Fèvre, O., Vettolani, G., Maccagni, D., et al. 2001, in Deep Fields, ed. S. Cristiani, A. Renzini, & R. Williams, Proc. of the ESO/ECF/STScI Workshop, 236
McCracken, H., Radovich, M., Bertin, E., et al. 2003, A&A, accepted
Pentericci, L., Fan, X., Rix, H.-W., et al. 2002, AJ, 123, 2151
Pettini, M., Rix, S., Steidel, C., et al. 2002, ApJ, 569, 742
Rhoads, J., Dey, A., Malhotra, S., et al. 2003, AJ, 125, 1006
Steidel, C., Adelberger, K., Giavalisco, M., Dickinson, M., & Pettini, M. 1999, ApJ, 519, 1
Tresse, L., Rola, C., Hammer, F., et al. 1996, MNRAS, 281, 847